



Computación y Sistemas

ISSN: 1405-5546

computacion-y-sistemas@cic.ipn.mx

Instituto Politécnico Nacional

México

Cuevas de la Rosa, Francisco Javier; Servin Guirado, Manuel
Neural Networks applied to 3D Object Depth Recovery
Computación y Sistemas, vol. 7, núm. 4, abril-junio, 2004, pp. 285-298
Instituto Politécnico Nacional
Distrito Federal, México

Available in: <http://www.redalyc.org/articulo.oa?id=61570407>

- How to cite
- Complete issue
- More information about this article
- Journal's homepage in redalyc.org

redalyc.org

Scientific Information System

Network of Scientific Journals from Latin America, the Caribbean, Spain and Portugal

Non-profit academic project, developed under the open access initiative

RESUMEN DE TESIS DOCTORAL

Neural Networks applied to 3D Object Depth Recovery *Aplicación de redes neuronales en la reconstrucción tridimensional de objetos*

Graduated: Francisco Javier Cuevas de la Rosa

Graduated on August 21, 2000

Centro de Investigaciones en Óptica, A.C.

Loma del Bosque 115, León, Guanajuato, México

CP. 37150

e-mail: fjcuevas@cio.mx

Advisor: Manuel Servin Guirado

Centro de Investigaciones en Óptica, A.C.

Loma del Bosque 115, León, Guanajuato, México

CP. 37150

e-mail: mservin@cio.mx

Abstract

In this work the application of neural networks (NNs) in tridimensional object depth recovery and structured light projection system calibration tasks is presented. In a first approach, a NN using radial basis functions (RBFNN) is proposed to carry out fringe projection system calibration. In this case the RBFNN is modeled to fit the phase information (obtained from fringe images) to the real physical measurements. In a second approach, a Multilayer Perceptron Neural Network (MPNN) is applied to phase and depth recovery from the fringe patterns. A scanning window is used as the MPNN input and the phase or depth gradient measurements is obtained at the MPNN output. Experiments considering real object depth measurement are presented.

Keywords: Neural networks, structured light projection systems, softcomputing, computer vision, optical metrology, fringe demodulation, depth recovery, phase measurement

Resumen

En este trabajo se presenta la aplicación de redes neuronales (RN) en la reconstrucción tridimensional de objetos y su utilización en tareas de calibración en sistemas de proyección de luz estructurada. En una primer propuesta, se establece una red neuronal que utiliza funciones de base radial (RNFB) útil para calibrar un sistema de proyección de franjas. En este caso la RNFB es modelada para ajustar la información de fase, obtenida de los imágenes de franjas a mediciones físicas reales. Se propone una segunda técnica que utiliza una red neuronal multicapas de perceptrones (RNMP) para la recuperación de fase y profundidad a partir de los patrones de franjas. En esta técnica se utiliza una ventana de análisis conteniendo subimágenes de los patrones de franjas. Esta subimagen es utilizada como entrada de la RNMP, obteniendo como salida las mediciones de los gradientes de fase o profundidad. Se presentan experimentos que aplican las técnicas propuestas para medir un objeto real.

Palabras Clave: Redes neuronales, sistemas de proyección de luz estructurada, computación suave, visión por computadora, metrología óptica, demodulación de franjas, recuperación de profundidad, medición de fase.

1. Introduction

In general, the image formation physics knowledge and understanding is required to develop algorithms in the computer vision area. There are many experimental approaches related to obtain object depth from 2D images. We can mention photographic and photometric stereoscopic techniques (Brooks, 1982; Cardenas-García, 1995; Coleman, 1984; Grosso, 1995; Horn, 1986; Koendrick, 1980; Pentland, 1984; Weinshall, 1990; Woodham, 1980), interferometric technique (Creath, 1988; Malacara, 1992; Reid, 1987; Robinson, 1993), and structured light projection techniques (Cuevas, 1999, 2000, 2002;

Li, 1997; Takeda, 1982; Zou, 1995), among others. In structured light projection techniques, the cosenoidal fringe projection is one of the most used techniques. This paper is related with the object depth recovery using fringe projecting and interferometric techniques. These kind of techniques are frequently used in real metrological applications such as optical shop testing (Malacara, 1992), robot vision (Horn, 1986), vibrational analysis (Robinson, 1993), stress analysis (Burch, 1982), biometric measurement (Takasaki, 1973), fracture measurement (Creath, 1988) and fluid dynamics (Trolinger, 1975). The fringe images and interferograms can be expressed mathematically as :

$$I(x, y) = a(x, y) + b(x, y) \cos(\omega_x x + \omega_y y + \phi(x, y)) + n(x, y), \quad (1)$$

where $a(x, y)$ is the background illumination, which is related to the light source power used in the experimental set-up, $b(x, y)$ is the amplitude modulation (e.g. this value in a fringe projection system is related to the surface reflectance of the object). The phase term $\phi(x, y)$ is related to the physical magnitude being measured. ω_x and ω_y are the angular carrier frequency in directions x and y . The term $n(x, y)$ is additive phase noise due to experimental conditions. Finally, we need to carry out a calibration process by means of a function (linear or non-linear), which maps unwrapped phase $\phi(x, y)$ with the real physical magnitude being measured.

The main purpose of the metrological techniques mentioned above is to apply digital image processing over the fringe images to approximate the phase term $\phi(x, y)$. There are different techniques used to quantify the phase term from fringes patterns. The spatial synchronous method (Ichioka, 1972; Womack, 1984a, 1984b), the Fourier method (Takeda, 1981, 1982, 1983), and the phase locked loop (PLL) (Servin, 1993a, 1994) are examples of these techniques. These analyse the digitized fringe pattern and detect the spatial phase variations due to the physical quantity being measured. In Spatial synchronous technique, the phase can be approximated by multiplying the fringe image by a sine and cosine function contains the same carrier frequency. Then, a low pass filter should be applied to eliminate the high frequency terms. If the ratio of both signals is calculated then the 2π wrapped phase of $\phi(x, y)$ is obtained. Finally, an unwrapping process should be applied to obtain the phase unwrapped field (Ghiglia, 1994; Servin, 1998, 1999). In such case the frequency cut-off threshold of the pass filter is difficult to be determined. On the other hand, in the Fourier transform method the phase term is approximated by using the Fast Fourier Transform (FFT). The fringe pattern is first transformed and a bandpass filter tuned on the spatial carrier frequency is applied. Then, the inverse FFT is applied to obtain the wrapped phase of $\phi(x, y)$. Finally, in the phase locked loop method the phase is estimated by following the phase changes of the input signal by varying the phase of a computer-simulated oscillator (VCO) such that the phase error between the fringe pattern and VCO's signal vanishes. In PLL method an adequate value for the gain loop parameter is required so that the method can work appropriately. These techniques return the phase map in radians so that a calibration procedure is required to obtain the real physical measurement. A drawback is that the explicit knowledge of the optical experimental set-up parameters is required to carry out the conversion of the phase term to real physical measurements, which is a difficult task.

In a conventional fringe projection metrological system (see Fig. 1) a monochromating grating is projected over a surface, which is placed in a reference plane. The reference plane is located a distance d_0 from the projection and detection system. The optical axes of the pinhole camera and the grating projector are parallels and separated in d_l units. The optical axes are normal to the reference plane. The geometrical origin is considered to be placed on the pinhole camera center and the z -axis is located along its optical axis. The reference plane is considered to be in a position $z(x, y) = 0$.

In the measurement process, a fringe image is captured from the fringe projection system. Then, a phase detection technique is applied to obtain the phase in radians. In the ideal case, the phase can be converted to depth ($z(x, y)$) conversion by the following analysis: The phase on a surface point C , ϕ_C , has the same value that the phase on a point A , ϕ_A . The point C on the surface and point B on the reference plane are detected by the CCD array at the same point B' . The distance AB is calculated as :

$$AB = \frac{\phi_B - \phi_C}{2\pi f}, \quad (2)$$

where f is the spatial frequency projected grating on the reference plane and the object test. ϕ_B is the detected phase on point B . Finally, the depth conversion for point C can be expressed as:

$$z(x, y) = \frac{(\phi_B - \phi_C)d_0}{2\pi d_1 + \phi_B - \phi_C} \quad (3)$$

This equation can be applied only when a pinhole camera is considered and the test surface is located far away from the fringe projector metrologic system. In general many calibration difficulties are presented when a real experimental set-up is used with optical components. Some of these calibration difficulties can be enumerate as follows: (1) The diverging fringe projection; (2) the digital camera perspective distortion; and (3) the use of crossed optical-axis geometry. These circumstances have non-linear effects on the recovered phase.

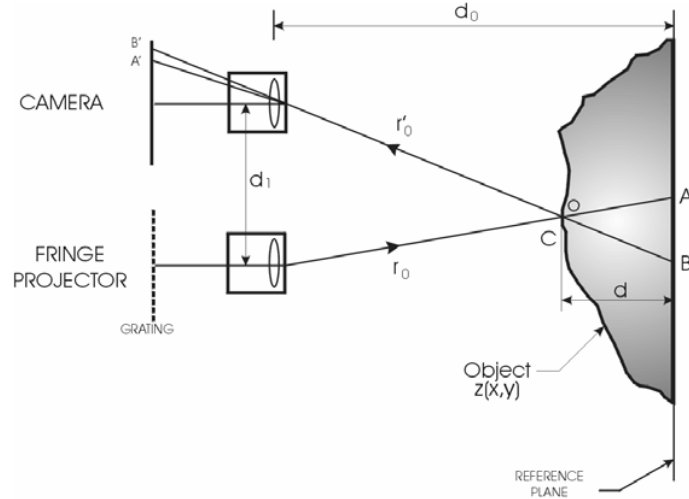


Fig. 1. A fringe projection metrologic system

In this work, we propose two approaches to solve the calibration problem and the object depth recovery. These approaches are based on applying Neural Networks (NN's). In a first approach, the main idea is to use a NN based on Radial Basis Functions (RBFNN) to make the conversion process of the recovered phase to real object depth data without explicit knowledge of the vision system parameters. In a second approach, it is proposed a calibration technique using a Multilayer Perceptron Neural Network (MPNN) that can approximate in a direct way the local depth gradient of the test surface from the local irradiance of the fringe image. The MPNN is used to demodulate open fringe patterns, but it can be extended to work with closed fringe patterns.

The work is organized in the following way. In section 2, the RBFNN technique used for calibration tasks is explained. In section 3, the MPNN technique is described to carry out depth recovery and calibration tasks, while in section 4 real experiments to approximate the measurements of a pyramidal object are shown. In section 5 future trends are posed. Finally, in section 6, conclusions are given.

2. Depth Object Recovery using Radial Basis Functions

In a first approach a neural network based in radial basis function (RBFNN) (Broomhead, 1988; Cuevas, 1999; Musavi, 1992; Powell, 1985; Servin, 1993) is proposed to carry out the phase to depth calibration process in a fringe projection metrologic system. The idea consists of obtaining the phase field from n reference calibration planes by using of conventional techniques such as Synchronous method, Fourier technique or Phase Locked Loop. The distorted phase field of each plane is used as input of the RBFNN and it is trained by weight calculation to obtain the depth desired position of the respective plane at the neural network output. RBFNNs are frequently used to carry out multivariate nonlinear mappings. An advantage of the RBFNN training is that it can be achieved in a high speed in comparison with backpropagation training.

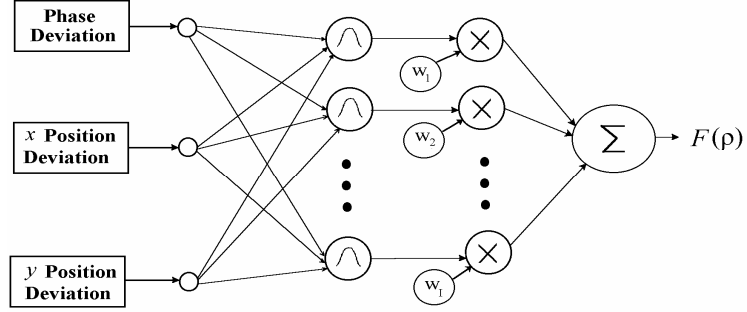


Fig. 2. RBFNN topology used in the calibration problem

The radial basis functions responds strongly near center of the neuron and its response decreases strongly to zero as the inputs ratios front centers increase. In this approach, Gaussian neurons and a two-layer topology are used (See Fig. 2). The centers of the RBF neurons are uniformly spaced within reference planes in the measurement volume. Then, the RBFNN works as an interpolation function of the phase field to the object depth field. The reference detected phase and the training set are obtained from a number of calibration planes. The phase field presents geometrical distortion due to the diverging fringe projection and the different perspective of the camera and fringe projection optics (crossed-optical-axis geometry). Then, the object depth field is approximated by fitting RBFNN weights of a linear combination of Gaussian functions. The Gaussian centers c_i are placed over samples of the dectected phases $\phi_p(x_i, y_i)$ obtained from P planes (see Fig. 3).

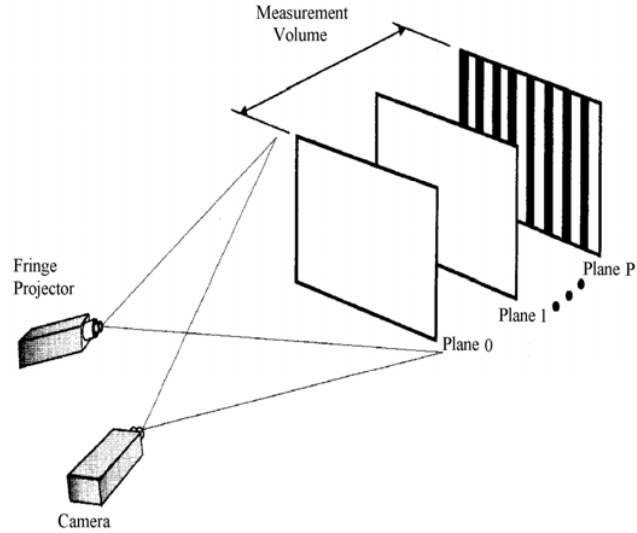


Fig. 3. Calibration planes in the fringe projection metrologic system

The Gaussian linear combination can be expressed as:

$$F(\mathbf{p}) = \sum_{i=1}^I w_i G_i(\mathbf{p}) \quad (4)$$

where

$$G_i(\mathbf{p}) = \exp\left[-\frac{\|\mathbf{p} - \mathbf{c}_i\|^2}{\sigma^2}\right], \quad (5)$$

and $\mathbf{p} = (\phi(x, y), x, y)$ and $\mathbf{c}_i = (\phi_p(x_i, y_i), x_i, y_i)$. \mathbf{p} is the feature or attribute vector that contains the detected and unwrapped phase $\phi(x, y)$ and its location point (x, y) . I is the total number of Gaussians kernels centered at \mathbf{c}_i . The weights w_i are the parameters of the RBFN to be calculated. Then, we need to minimize the total quadratic error defined as

$$E = \sum_{j=1}^J [F(\mathbf{p}_j) - h_j]^2, \quad (6)$$

where J training pairs are considered as the set to fit the weights. The function F is the best linear combination of Gaussian that adjust the experimental depth field and therefore it minimize the error function E . The best RBFNN parameters are found by derivating error function with respect to weights and make it equal to zero. This can be mathematical expressed as:

$$\frac{\partial E}{\partial w_k} = \sum_{j=1}^J \left[\sum_{i=1}^I w_i G_i(\mathbf{p}_j) - h_j \right] G_k(\mathbf{p}_j) = 0, \quad (7)$$

$$\forall (k = 1, 2, 3, \dots, I).$$

or it can be arranged as a matrix equation system as follows,

$$\Lambda W = \Omega, \quad (8)$$

where

$$\Lambda = [\lambda_{ki}] = \left[\sum_{j=1}^J G_k(\mathbf{p}_j) G_i(\mathbf{p}_j) \right], \quad (9)$$

$$\forall (k, i = 1, 2, 3, \dots, I)$$

$$W^T = (w_1, w_2, \dots, w_I), \quad (10)$$

and

$$\Omega_k = \sum_{j=1}^J G_k(\mathbf{p}_j) h_j, \quad (11)$$

$$\forall (k = 1, 2, 3, \dots, I)$$

Finally, the equation system is solved by pre-multiplying both sides of $\Lambda W = \Omega$ by Λ^{-1} and the optimum weights are obtained.

3. Multilayer Perceptron Neural Network applied to Phase and Depth Recovery

In a second proposed technique, a three-layer Perceptron Neural Network (Cuevas, 2000; Grossberg, 1998; Kenue, 1991; Mills, 1995; Minsky, 1969; Rumelhart, 1986; Wasserman, 1989) is applied to solve the calibration and depth recovery problem. The MPNN is shown in Fig. 4. The training set S is formed by pair vectors $(s_{x,y})$ which contain a subset of sub images $(W(x, y))$ and its related local directional depth gradients $(\Delta z(x, y))$. These sub images are obtained from fringe patterns projected over a surface test or an interferogram come from a previous calibrated object (see Fig. 5). Then each point (x, y) in the fringe image has a related training pair vector $s_{x,y}$, that is:

$$S = \bigcup_{x=1}^X \bigcup_{y=1}^Y s_{x,y} m(x, y), \quad (12)$$

where

$$s_{x,y} = [W(x, y), \Delta z(x, y)], \quad (13)$$

and

$$\Delta z(x, y) = \left(\frac{\partial z(x, y)}{\partial x}, \frac{\partial z(x, y)}{\partial y} \right), \quad (14)$$

where X and Y are the number of rows and columns of the training fringe image, respectively. $W(x,y)$ is formed from the irradiance values obtained of a $M \times M$ neighborhood scanning window centered around pixel (x,y) of the real fringe image or interferogram related to the test object. The function $m(x,y)$ is a binary mask which considers the valid area inside of the fringe image. $m(x,y)$ is set with 1 if pixel in (x,y) is a valid pixel and 0 otherwise. The depth directional gradients are approximated by differences in the directions x and y . These can be written as :

$$\begin{aligned} \frac{\partial z(x, y)}{\partial x} &\approx \Delta z_x(x, y) = \Delta z_1(x, y) \\ &= \frac{z(x, y) - z(x-1, y)}{\rho}, \end{aligned} \quad (15)$$

$$\begin{aligned} \frac{\partial z(x, y)}{\partial y} &\approx \Delta z_y(x, y) = \Delta z_2(x, y) \\ &= \frac{z(x, y) - z(x, y-1)}{\rho}, \end{aligned} \quad (16)$$

where $z(x,y)$ represents height obtained from the calibration object. These depth fields are normalized in the range $[0,1]$ using the constant ρ . Then, the MLNN should be trained by adjusting MPNN weights to minimize the following error function :

$$U_{\Delta z} = \sum_{x=1}^X \sum_{y=1}^Y \left[(\Delta z_x(x, y) - \Delta \tilde{z}_x(x, y))^2 + (\Delta z_y(x, y) - \Delta \tilde{z}_y(x, y))^2 \right] m(x, y), \quad (17)$$

$\Delta \tilde{z}_x(x, y)$ and $\Delta \tilde{z}_y(x, y)$ are the two-outputs of the MPNN which estimate the depth gradients at point (x,y) and $m(x,y)$ is the binary mask where data are valid.

The MPNN should be trained by adjusting weights to achieve the minimization of the error function. Then, the following neural network output notation is established to do the mathematical analysis :

$$O_q^p = \sum_{k=1}^N w_{kq}^p I_k^p, \quad (18)$$

and

$$I_k^p = \frac{1}{1 + e^{-O_k^{p-1}}}, \quad (19)$$

where I_k^p is the input to the p -th layer from k -th neuron of the $p-1$ layer, w_{kq}^p is the weight of the k -th neuron in the $p-1$ layer with the q -th neuron in the p -th layer, and O_q^p is the intermediate/unthresholded output of the q -th neuron in the p -th layer. Then, the error function can be optimized by step gradient descent method. This is carried out by the following output layer weight fitting:

$$w_{jk}^s(t+1) = w_{jk}^s(t) + \eta \frac{\partial U_{\Delta z}}{\partial w_{jk}^s}, \quad (20)$$

$$j \in [1, J], k \in [1, 2],$$

where

$$\frac{\partial U_{\Delta z}}{\partial w_{jk}^s} = (\Delta z_k(x, y) - \Delta \bar{z}_k(x, y)) \frac{\partial \Delta h_k}{\partial w_{jk}^s} \text{sigm}(O_j^q), \quad (21)$$

and

$$\frac{\partial \Delta h_k}{\partial w_{jk}^s} = \text{sigm}(O_k^s) [1 - \text{sigm}(O_k^s)], \quad (22)$$

w_{jk}^s are the weights in the output layer. O_j^q, O_k^s are the neural outputs in the hidden (superscript q) and output (superscript s) layers, respectively. η is the learning rate that determines the size of the step in the minimization algorithm. For the weights in the hidden layer w_{ij}^q , the fitting equations can be expressed as:

$$w_{ij}^q(t+1) = w_{ij}^q(t) + \eta \frac{\partial U_{\Delta z}}{\partial w_{ij}^q}, \quad (23)$$

$$i \in [1, R], j \in [1, J],$$

with

$$\frac{\partial U_{\Delta z}}{\partial w_{ij}^q} = \frac{\partial \text{sigm}(O_j^q)}{\partial w_{ij}^q} I_i \sum \delta_k^s w_{jk}^s, \quad (24)$$

and

$$\delta_k^s = (\Delta z_k(x, y) - \Delta \bar{z}_k(x, y)) \frac{\partial \Delta h_k}{\partial w_{jk}^s}. \quad (25)$$

Then, the weight fitting procedure should be iterated until average error reaches a tolerance value. The average error μ defined in the problem can be expressed as:

$$\mu = \frac{1}{T} \sum_{x=1}^X \sum_{y=1}^Y \left(\left| \frac{\Delta z_x(x, y) - \Delta \bar{z}_x(x, y)}{\Delta z_x(x, y)} \right| + \left| \frac{\Delta z_y(x, y) - \Delta \bar{z}_y(x, y)}{\Delta z_y(x, y)} \right| \right) m(x, y) \quad (26)$$

where T is the number of valid pixels inside $m(x, y)$.

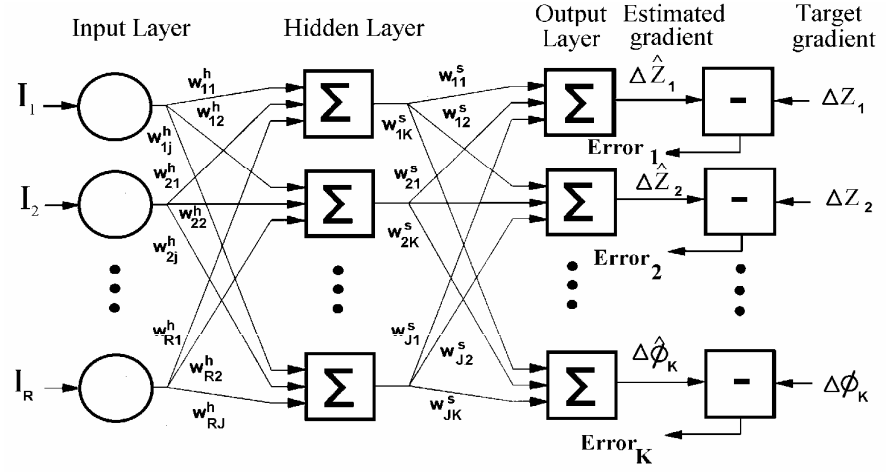


Fig. 4. MPNN used in the phase and depth object recovery problem

Finally, the estimated depth gradients should be integrated using a relaxation method. In this case, the following error function should be minimized:

$$U_f = \sum_{(x,y)} \left\{ [\hat{f}(x,y) - f(x-1,y) - \Delta z_x(x,y)]^2 + [\hat{f}(x,y) - f(x,y-1) - \Delta z_y(x,y)]^2 \right\} \times m(x,y) \quad (27)$$

$\hat{f}(x,y)$ is the surface that best fits the estimated gradient field $\Delta \bar{z}(x,y)$. Function U_f can be optimized by gradient descent by using the following expression:

$$\hat{f}^{t+1}(x,y) = \hat{f}^t(x,y) - \alpha \frac{\partial U_f}{\partial \hat{f}(x,y)} \quad (28)$$

where α is the step in the optimization procedure. The process is iterated until a tolerance is reached.

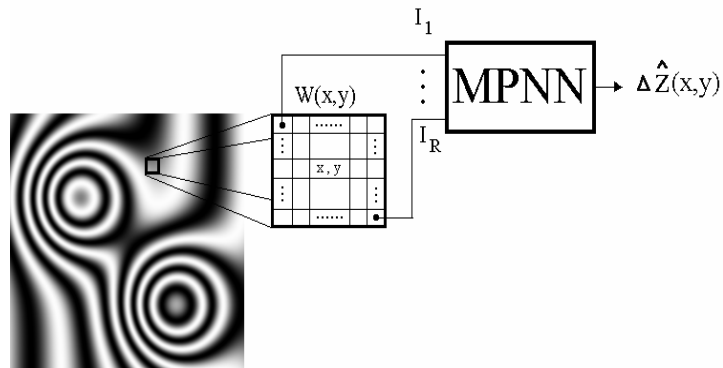


Fig. 5. Scanning window used as MPNN input in the phase and depth recovery process

4. Experiments

The performance of the proposed neural networks (MPNN and RBFNN) was tested in a real experiment where a pyramidal object was measured. In both cases a fringe projection system was used to obtain fringe images. A Ronchi grating was placed in a Kodak Ektagraphic slide projector with a $f/3.5$ zoom lens. Fringes images were captured with a resolution of 256×256 pixels. In a first experiment, a pyramidal object was measured by means of the RBFNN technique. Three images coming from three different calibration planes were digitized. The reference planes were placed at $z=0$, 3 and 6 cm. In this case the PLL technique was used to calculate the unwrapped phase field of the fringe images. Then, a RBFNN with 75 Gaussian processors was used for depth field. A standard deviation value of 8.0 was used in each Gaussian processor. Fig. 6 shows the pyramidal object fringe image and Fig. 7 depicts a graph of the distorted recovered phase field. Fig. 8 shows the depth field conversion using the RBFNN. The average error using RBFNN was 0.13 cm.

In the second case an hemispherical calibration object was used to obtain the training set. This object was measured using a ZEISS CMM C400 machine. The MPNN was trained until a 0.5 % average error was reached. In Fig. 9 the fringe pattern projected over the hemispherical calibration object is shown. Then the fringe image of a pyramidal object was used to measure it by using the MLNN technique. The full measurement graph is shown in Fig. 10. For this case the average error in the measurement was 0.088 cm.

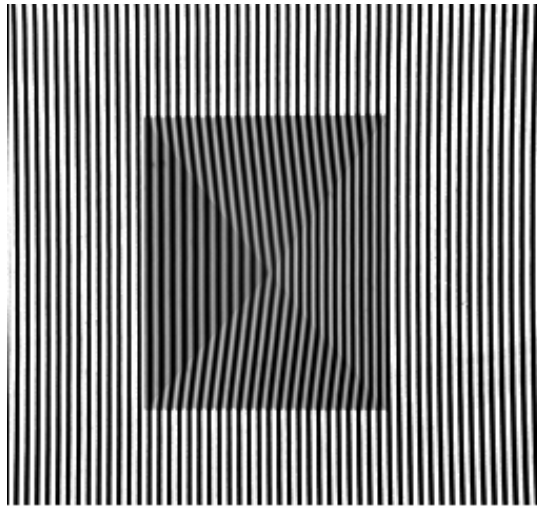


Fig. 6. Fringe projection over the pyramidal object

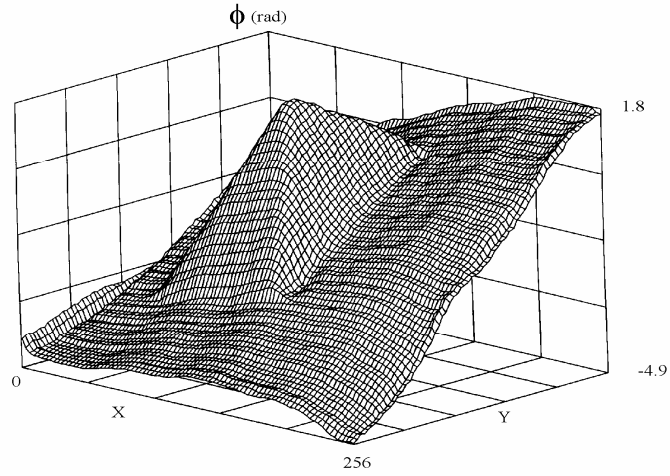


Fig. 7. The phase field obtained from Figure 6 using PLL technique

5. Future trends

In previous sections, two approaches of neural networks were proposed to carry out phase to depth conversion tasks. Currently, we have been working with another artificial intelligence and softcomputing techniques. In this case the Genetic Algorithms (GAs) have been a good tool to demodulate phase from fringe patterns.

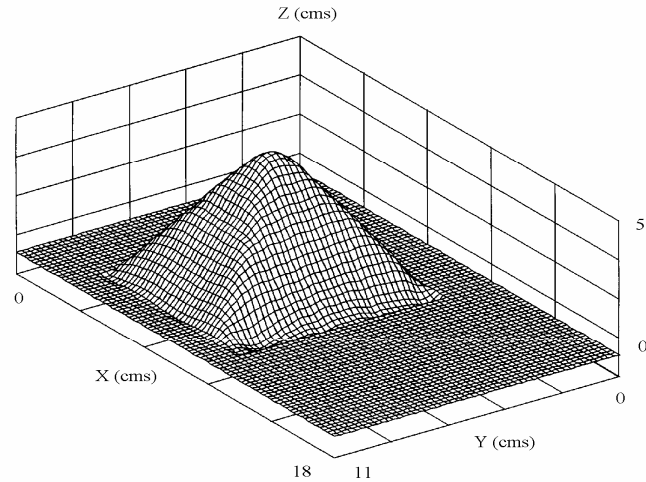


Fig. 8. Depth field recovered using the RBFNN technique

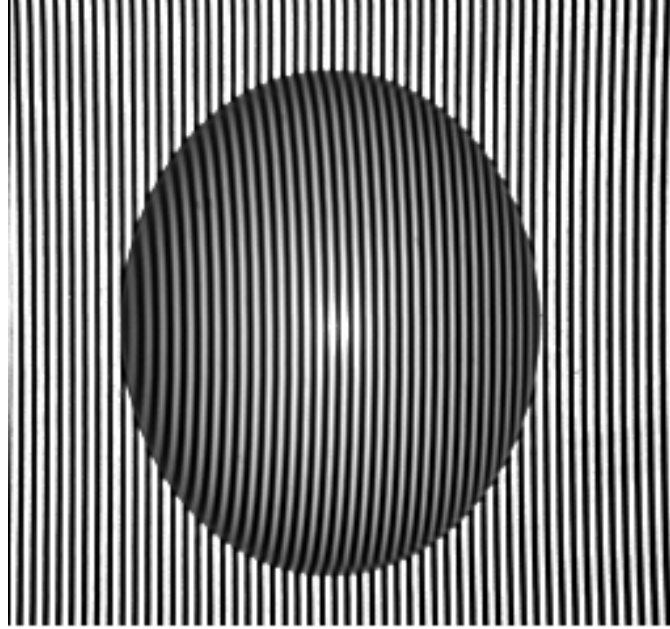


Fig. 9. Fringe projection over the training hemispherical object

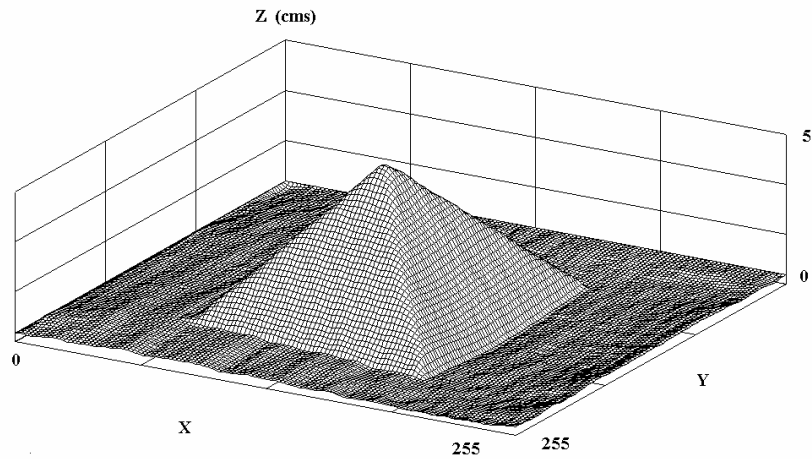


Fig. 10. Depth measurement of a pyramidal object using the MPNN technique

The main idea is to optimize a regularized fitness function which models the phase demodulation problem. This function considers *a-priori* knowledge about the demodulation problem, to fit a non-linear function. The *a-priori* knowledge considered can be enumerate in the following way: a) the closeness between the observed fringes and the recovered fringes b) the phase smoothness, and c) prior knowledge of the object as its shape and size. Results of the GA technique can be founded in Cuevas (2002). Future trends includes the hardware implementation of the proposed techniques.

6. Conclusions

In this work, two neural network approaches were proposed to carry out depth recovery and calibration tasks. These techniques can be applied to fringe projection images and/or fringe images coming from interferometers. In a first approach, a Radial Basis Function Neural Networks (RBFNN) is applied to convert the phase field to depth object field. The RBFNN technique corrects the geometrical distortion of the recovered unwrapped phase caused by the diverging illumination of the slide projector, the perspective distortion of the optical system of the digital camera and the non-linear calibration of the crossed-optical geometry used. In such case, the RBFNN works as an interpolation function to approximate the object depth field starting from the reference calibration planes. In the second case, a Multilayer Perceptron Neural Network (MPNN) was applied to object depth recover starting from a fringe sub-image. A fringe image and depth gradients coming from calibration object are used as training set. A scanning window was used as the MPNN input and the depth directional gradients are obtained in MPNN output. These are integrated by a relaxation method to obtain the full object depth field. An advantage of both cases is that a knowledge of the optical parameters is not required.

Analyzing the performance of the approaches, it can be pointed out that the MPNN approach has a better average error performance. This is due to different reasons such as phase demodulation applied technique, low-pass used filter in the phase demodulation and training set, among others. This is explained in the extense work.

Future trends considers the application of other artificial intelligence and softcomputing techniques such as Genetic Algorithms and Fuzzy Logic, besides of the hardware implementation of the proposed techniques.

Acknowledgements

The author would like to thank Dr. Jose Luis Marroquin, Dr. Fernando Mendoza, Dr. Ramón Rodríguez Vera, Dr. Orestes Stavroudis, and Raymundo Mendoza for the invaluable technical and scientific support in the development of this work. We also acknowledge the support of the Consejo Nacional de Ciencia y Tecnología de México, Consejo de Ciencia y Tecnología del Estado de Guanajuato, and Centro de Investigaciones en Óptica, A.C.

References

1. **Burch, J.M., Forno, C.**, "High resolution moire photography", *Opt. Eng.*, Vol. 21, 1982, pp. 602-614
2. **Bone, D.J.**, "Fourier fringe analysis : the two-dimensional phase unwrapping problem", *Appl. Optics*, Vol. 30, 1991, pp. 3627-3632,
3. **Broomhead D. S. and Lowe D.**, "Multivariable functional interpolation and adaptive networks", *Complex Systems*, Vol. 2, 1988, pp. 321-355.
4. **Brooks, M. J.**, " Shape from Shading Discretely", Ph.D. Thesis. Essex Univ., Colchester, England., 1982
5. **Cuevas, F.J., M.Servin, R. Rodríguez-Vera**, "Depth object recovery using radial Basis Functions", *Opt. Comm.*, Vol. 163, 1999, p.270
6. **Cuevas, F.J., M. Servin, O.N. Stavroudis, R. Rodríguez-Vera**, "Multi-Layer neural network applied to phase and depth recovery from fringe patterns", *Opt. Comm.*, Vol. 181, 2000, pp. 239-259
7. **Cuevas, F.J., J.H. Sossa-Azuela, M. Servin**, "A parametric method applied to phase recovery from a fringe based on a genetic algorithm", *Opt. Comm.*, Vol. 203, 2002, pp. 213-223
8. **Cardenas-Garcia, J.F., and Yao, H. , and Zheng, S. ,** 3D reconstruction of objects using stereo imaging , *Opt. and Lasers in Engineering*, Vol. 22, 1995, p. 192-213
9. **Coleman E. and Jain R.**, " Obtaining 3-Dimensional Shape of Textured and Specular Surfaces Using Four- Source Photometry", *Comp. Graph.*, Vol. 18, 1984, pp. 309-328.
10. **Creath, K.**, " Phase measurement interferometry techniques", in *Progress in Optics*, Ed. E. Wolf, Vol. XXVI de Elsevier Science Publishers B.V., 1988, pp. 348-393.
11. **Freeman, J. and Skapura, D.** *Neural networks : Algorithms, Applications & Programming Techniques.*, Addison-Wesley Publishing Company, 1991
12. **Ghiglia, D.C. and Romero, L.A.**, Robust two-dimensional weighted and unweighted phase unwrapping that uses fast transforms and iterative methods, *J. Opt. Soc. Am. A*, Vol. 11, 1994, pp 107-117
13. **Grossberg, S.**, "Non-Linear Neural Networks : Principles. Mechanisms, and Architecture", *Neural Networking*, 1988, Vol. 1, pp. 17-61

14. **Grosso, E. and Tistarelli, M.**, Active/Dynamic stereo vision, *IEEE Trans. Patt. Analysis And Mach. Intelligence*, vol. 17, 1995, pp. 868-879
15. **Horn, B.K.P.**, *Robot Vision*, Ed. Mc Graw Hill, New York, 1986.
16. **Ichiooka Y. and Inuiya M.**, "Direct phase detecting system", *Appl. Optics*, Vol. 11, 1972, pp.1507-1514.
17. **Joenathan, C. and Khorana, M.** Phase measurement by differentiating interferometric fringes, *Journal of Modern Optics*, Vol. 39, 1992, pp. 2075-2087
18. **Kenue, S.K.**, "Efficient activation Functions for the Back-Propagation Neural Network", *Intelligent Robots and Computer Vision X. SPIE Vol.1608*, 1991, pp. 450-456 .
19. **Koenderink, J.J. and A.J. van Doorn**, " Photometric Invariants Related to Solid Shape", *Acta Optica*, Vol. 27, 1980, pp. 981-996.
20. **Kozlowski, J., Serra, G.**, New modified phase locked loop method for fringe pattern demodulation, *Opt. Eng.* , Vol. 36, 1997, pp. 2025-2030
21. **Li, J. , Su, X., Guo, L.**, Improved Fourier transform profilometry for the automatic measurement of three-dimensional object shapes, *Opt. Eng.*, Vol. 29, 1990, pp. 1439-1444
22. **Li, J., Su, H., Su, X.**, Two-frequency grating used in phase profilometry, *Appl. Opt.*, Vol. 36, 1997, pp. 277-280
23. **Lin, J. and Su. X.**, Two-dimensional Fourier transform profilometry for the automatic measurement of three dimensional object shapes, *Opt. Eng.*, Vol. 34, 1995, pp. 3297-3302
24. **Malacara D.** Editor, *Optical Shop Testing*, John Wiley & Sons, Inc, New York, 1992
25. **Mills, H. , Burton, D. R. , Lalor, M.J.** , Applying backpropagation neural networks to fringe analysis, *Optics and Lasers in Engineering*, Vol. 23, 1995, pp. 331-341
26. **Minsky, M and Papert, S.**, *Perceptrons*, MIT Press, Cambridge, MA., 1969
27. **Musavi, M., Ahmed, W, Chan k., Faris, K., Hummels, D.**, "On training of radial basis functions classifiers", *Neural Networks*, Vol. 5, 1992, pp. 595-603.
28. **Pentland A.P.**, "Local Shading Analysis", *IEEE Trans. on Pattern Analysis and Machine Intelligence*, Vol. 6 , 1969, pp. 170-187.
29. **Powell, M.J.D.**, Radial basis functions for multivariate interpolation : a review. In M. G. Cox & J. C. Mason (Eds.) , *Algorithms for the approximation of functions and Data*. New York: Oxford University Press, 1985
30. **Reid, G.T.**, Automatic fringe pattern analysis : A review, *Optics and Lasers in Engineering*, Vol. 7, 1987, pp. 37-68
31. **Robinson, D.W. and Reid, G.T.**, *Interferogram Analysis : Digital Fringe Measurement Techniques*, Institute of Physics Publishing, London, England, 1993
32. **Roddier, C. and F. Roddier**, "Interferogram analysis using Fourier transform techniques", *Appl. Opt.*, Vol. 26, 1987, pp. 1668-1673 .
33. **Rodriguez-Vera, R. and Servin, M.**, Phase locked loop profilometry, *Optics and Laser technology*, Vol. 26, 1994, 393-398
34. **Rumelhart, D.E., Hinton G.E. and Williams. R.J.**, " Learning internal representations by error propagation". *Parallel Distributed Processing : Explorations in the Microstructures of Cognition*, Vol 1, D.E. Rumelhart and J.L. McClelland (Eds.) Cambridge, MA : MIT Press, 1986, pp. 318-362.
35. **Sandoz, P.**, High-resolution profilometry by using phase calculation algorithms for spectroscopy analysis of white-light interferograms, *Jour. of Modern Opt.*, Vol. 43, 1996, pp. 701-708.
36. **Servin, M. and R. Rodriguez-Vera**, "Two dimensional phase locked loop demodulation of interferograms", *Journ. of Modern Opt.* Vol. 40, 1993a, pp 2087-2094.
37. **Servin, M. and Cuevas, F.J.**, " A new kind of neural network based on radial basis functions", *Rev. Mex. Fis.*, Vol. 39, 1993, pp. 235-249.
38. **Servin, M., Malacara, D. , Cuevas, F.J.**, Direct-phase detection of modulated Ronchi rulings using a phase-locked loop , *Opt. Eng.*, Vol. 33, 1994, pp. 1193-1199
39. **Servin, M. and Cuevas, F.J.**, , A novel technique for spatial phase-shifting interferometry, *Jour. of Modern Optics*, Vol. 42, 1995, pp. 1853-1862
40. **Servin, M. , Marroquin, J.L. , Malacara, D., Cuevas, F.J.** , Phase unwrapping with a regularized phase-tracking system, *Appl. Optics*, Vol. 37, 1998, pp. 1917-1923
41. **Servin, M. , F.J. Cuevas, D. Malacara, J.L. Marroquin, R. Rodriguez-Vera**, Phase unwrapping through demodulation by use of the regularized phase-tracking technique, *Appl. Optics*, Vol. 38, No. 10, 1999, pp. 1934-1941
42. **Takasaki, H.**, "Moire Topography", *Applied Optics*, Vol. 12, 1973, pp. 845-850
43. **Takeda, M., Ina, H., Kobayashi, S.**, Fourier-transform method of fringe-pattern analysis for computer-based topography and interferometry, *Journal of Optical Soc. of America*, Vol. 72, 1981, pp. 156-16
44. **Takeda, M., H. Ina, and S. Kobayashi.**, "Fourier transform methods of fringe- pattern analysis for computer-based topography and interferometry", *J. Opt. Soc. Am.*, Vol. 72, 1982, pp.156-160.
45. **Takeda, M. and K. Mutoh**, "Fourier transform profilometry for the automatic measurement of 3-D object shapes", *Appl. Opt.*, Vol. 22, 1983, pp. 3977-3982.
46. **Trolinger, J.D.**, "Flow visualization holography", *Opt. Eng.*, Vol. 14, 1975, 470-481
47. **Wasserman, P.D.**, Backpropagation, Chap. 3 in *Neural computing* , Van Norstrand Reinhold, New York, 1989
48. **Weinshall, D.**, Qualitative depth from stereo with applications, *Computer Vision, Graph. and Image Processing*, Vol. 49, 1990, p.222-241.

Francisco J. Cuevas de la Rosa y Manuel Servin Guirado

49. **Womack, K. H.**, "Interferometric phase measurement using spatial synchronous detection", *Opt. Eng.*, Vol. 23, 1984a, pp. 391-395
50. **Womack, K. H.**, " Frequency domain description of interferogram analysis", *Opt. Eng.*, Vol. 23, 1984b, pp. 396-400 .
51. **Woodham, K. H.**, "Photometric method for determining surface orientation from multiple images", *Opt. Eng.*, Vol. 19, 1980, p.139
52. **Zou, D. , Ye , S., and Wang , Ch. ,** Structured-lighting surface sensor and its calibration, *Opt. Eng.*, Vol. 34, No.10, 1995, pp. 3040-304



Francisco Javier Cuevas de la Rosa. Received his BS degree in Computer Systems Engineering from Instituto Tecnológico y de Estudios Superiores de Monterrey (ITESM) Campus Monterrey in 1984. He obtained his Master degree in Computer Science from ITESM Campus Edo. de México in 1995 and his PhD in Optics Metrology from Centro de Investigaciones en Óptica, A.C. in 2000, where he is currently a researcher. He made a postdoctoral stay in Centro de Investigación en Computación of Instituto Politécnico Nacional of México, between 2001 and 2002. He has more than 20 publications in international journals with rigorous refereeing and more than 40 works in national and international conferences. He is a member of the Sistema Nacional de Investigación (SNI) of México since 1995. His research lines cover: Optical Metrology, Computer Vision, Digital Image Processing, Pattern recognition, Neural Networks and Genetic Algorithms.



Manuel Servin Guirado. His undergraduate studies were in Electrical Communication Engineering at the University of Guanajuato, Mexico. He then pursued graduate studies in France at the Ecole Nationale Supérieure des Telecommunications Br. (ENST) obtaining a Diplôme d'Ingenieur. He then enters the CIO in Leon, as research assistant for about 10 years and later on he spent a year at Motorola Corporation as designer engineer in microwave projects. After that, he enrolled as Doctoral student at the CIO where he obtained his Doctorado en Ciencias (Optica) in 1994, by the University of Guanajuato, Mexico. He is a level member III of Sistema Nacional de Investigación (SNI) of the CONACYT. Dr. Manuel Servin has been working since 1992 mainly in fringe processing algorithms or interferometry, and has supervised several Master and Doctoral students.